Geosynthetics 2009
February 25-27 2009, Salt Lake City, Utah

Location of Failure Plane within Narrow GRS Wall Systems

Kuo-Hsin Yang, Dept.of Civil Architectural and Environmental Engineering, Univ.of Texas at Austin, TX, USA
Ranjiv Gupta, Dept.of Civil Architectural and Environmental Engineering, Univ.of Texas at Austin, TX, USA
J.G. Zornberg, Dept. of Civil Architectural and Environmental Engineering, Univ. of Texas at Austin, TX, USA

ABSTRACT
The design of a Geosynthetic Reinforced Soil (GRS) wall for internal stability requires computing the reinforcement embedment length against pullout failure. The location of failure plane is important input for this design. The current FHWA design guidelines assume the location of failure plane based on Rankine theory. While this assumption holds true for conventional walls it is unconservative for GRS walls under constrained spaces, also known as "narrow GRS walls". The observations from centrifuge tests suggest that the inclination angle of failure plane is less than that one calculated based on Rankine theory for narrow GRS walls. This paper presents a limit equilibrium study to accurately locate failure planes within narrow GRS walls. The critical failure planes within narrow GRS walls are searched using Spencer's method with a function of noncircular failure plane. The results predicted from limit equilibrium analyses shows a good agreement with the experimental data from centrifuge tests conducted on narrow walls. The results indicate that critical failure plane is bilinear: the failure surface being formed partially through the reinforced soil and partially along the interface between the GRS and stable wall faces. Finally, the effect of wall aspect ratio on the inclination angle of the critical failure plane is computed and depicted in a chart for design purposes.

1. INTRODUCTION

The increase of traffic demands in urban areas has led to widening of existing highways. A possible solution to increase right of way is by constructing Geosynthetic Reinforced Soil (GRS) walls adjacent to previously stabilized walls. The acceptance of GRS walls as a viable solution has been driven by a number of factors, including aesthetics, reliability, cost, construction techniques, seismic performance, and the ability to tolerate large deformations without structural distress. However, due to the high cost of additional right of way and limited space available at job sites, construction of these GRS walls is done under a constrained space. This leads to GRS walls narrower than those recommended in current design guidelines. Narrow GRS wall systems are referred as a geosynthetic reinforced soil wall having an aspect ratio, *L/H*, (ratio of wall width, *L*, to wall height, *H*) less than 0.7 suggested in FHWA MSE wall design guidelines (Elias *et al.*, 2001) and placed in front of an existing stable wall (or shored wall). A "narrow" GRS wall systems used for widening of an existing highway is shown in Fig.1.

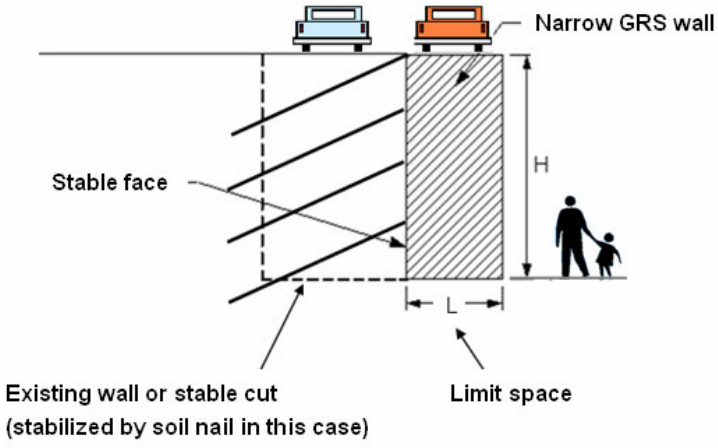

Figure 1: A narrow GRS wall system for widening of existing highway

The behavior of narrow GRS walls differs from those of conventional walls in terms of its interaction with the stable wall face, the magnitude of earth pressures, the location of failure planes and the failure mechanisms. Woodruff (2003) performed a comprehensive series of centrifuge model tests on narrow GRS wall systems. Woodruff (2003) observed that the failure planes of narrow walls was bilinear and had an inclination angle less than that of theoretical Rankine linear failure plane (*i.e.* $45+\phi/2$, ϕ is friction angle of backfill). A detailed description of Woodruff's centrifuge tests and results is presented in Section 2.

Currently, the MSE wall having aspect ratios ranging from 0.3 to 0.7 are designed based on FHWA design guidelines for Shored Mechanically Stabilized Earth (SMSE) wall systems (Morrison *et al.*, 2006). These guidelines deals with the uncertainties of narrow wall design by increasing the factor of safety, *FS*, rather than considering the actual characteristics of narrow walls. The FHWA SMSE wall design guidelines suggests to use Rankine failure plane for narrow walls but increase the *FS* against pullout from 1.5 to 2.0 for $L/H<0.4$.

The purpose of this paper is to provide better understanding regarding the behavior of narrow walls in terms of predicting the location of failure plane. The centrifuge tests reported in Woodruff's (2003) are analyzed; then the limit equilibrium modeling centrifuge testing on narrow walls is discussed with emphasis on the method for modeling reinforcement force and searching for nonlinear failure plane; third, the calculated results from limit equilibrium analyses are compared to the experimental data from centrifuge tests; finally, the design charts for variation in inclination angle of failure plane with wall aspect ratio is provided for design purposes.

2. CENTRIFUGE MODEL

A series of centrifuge model tests on reinforced soil walls adjacent to a stable face was performed by Woodruff (2003). A total of 24 different walls with *L/H* ranging from 0.17 to 0.9 were tested. All the reduced-scale walls were 230 mm high and the wall facing batter was 11 vertical to 1 horizontal. Monterey No. 30 sand was used as the backfill material with unit weight of 16 kN/m^3. The friction angle was interpolated from a series of triaxial compression tests (Zornberg, 2002) corresponding to the targeted backfill relative density of 70% as 36.7°. The estimated plane strain friction angle was reported as 42.2° using the correlations between triaxial friction angle and plane strain friction angle reported by Zornberg *et al.* (1998). The two different types of reinforcements used in centrifuge study were the commercially available nonwoven geotextiles: Pellon True-grid and Pellon Sew-in. Pellon True-grid was a white 60% polyester and 40% rayon fabric with mass per unit area of 28 g/m^2. The fabric, tested by wide width strip tensile tests (ASTM D4595), had strength of 0.09 kN/m in the machine direction and 1.0 kN/m in the transverse direction and referred as R2 and R4, respectively. Pellon Sew-in was a white 100% polyester fabric with a unit weight of 24.5 g/m^2. The fabric had strength of 0.03 kN/m in the machine direction and 0.1 kN/m in the transverse direction and referred as R1 and R3, respectively. The model walls were placed in front of the wall of aluminum strong box to simulate the stable face.

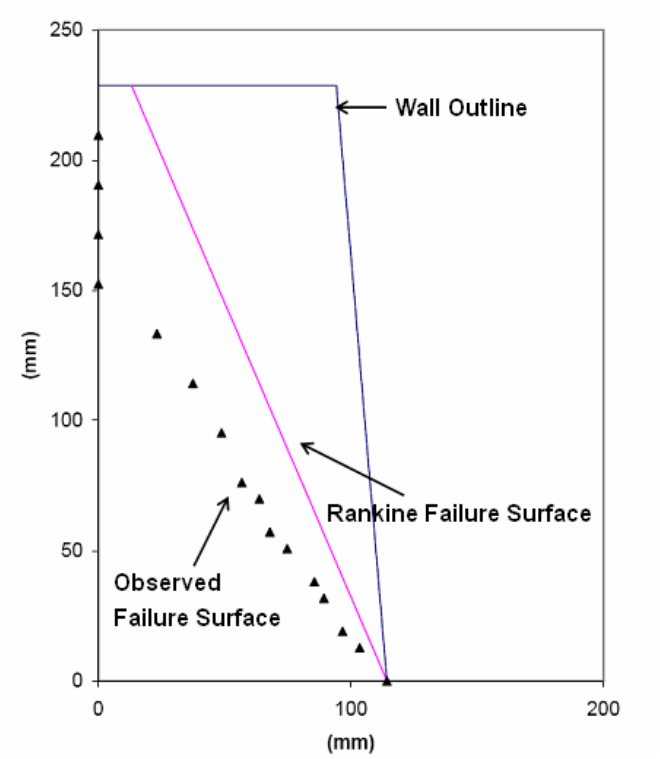

Figure 2. Compound failure at Test 2b, *L/H*=0.4 (Woodruff, 2003)

Tests were performed with above geotextiles involving five different vertical spacing layouts. Each wall was loaded to failure and acceleration (g) required to fail the wall was recorded. High-speed video cameras were used to record the deformations of the wall. The location of the failure surface was determined based on the observed tears (rupture) in each layer of the reinforcement. The tests indicated that the wall would fail internally at *L/H* >0.25 and fail externally in overturning mode at *L/H* < 0.25. For walls with *L/H* >0.6, the internal mode of failure occurred when weaker reinforcement (Pellon Sew-in) was used and no failure occurred with stronger reinforcement (Pellon True-grid). The critical failure planes were linear and the failure surface passed through entire reinforced soil area. When *L/H* ranged between 0.6 and 0.25, the wall failed internally in compound mode. Figure 2 shows the compound failure for a narrow MSE wall with *L/H*=0.4. The critical failure planes in compound failure were bilinear; the failure surface formed partially through the reinforced soil and partially along the interface between the MSE and stable wall faces. The inclination angle of failure plane was less than that predicted by theoretical Rankine failure plane.

3. LIMIT EQUILIBRIUM MODEL

The analyses presented in this section were conducted using limit equilibrium. The UTEXAS4 program developed by Dr. Stephen Wright at University of Texas at Austin (Wright 1999) was used. The primary reason for selecting Limit Equilibrium (LE) was due to their ability to accurately predict failure mechanisms in narrow MSE walls. LE method was used to model three centrifuge tests: Test 2a (L/H=0.6), Test 2b (L/H=0.4) and Test 3a (L/H=0.7). A summary of the condition and result of these tests is listed in Table 1. Since similar procedures are followed in the three tests, only the description of Test 2b is discussed in detail.

Table 1. Summary of centrifuge test conditions for limit equilibrium modeling

Test	Aspect Ratio	Reinforcement Strength	Failure Mode	Failure g-level	Reinforcement Spacing (mm)
2a	0.6	R2	Compound	39	20
2b	0.4	R2	Compound	41	20
3a	0.7	R2	Internal	38	20

3.1 Modeling of GRS and Stable Walls

Figure 3 shows the LE model of wall Test 2b. The geometry of wall model follows the dimension reported by Woodruff (2003), *i.e*, wall height of 230 mm, wall aspect ratio of 0.4 at top of the wall, wall face batter 11 vertical to 1 horizontal, and twelve layers of reinforcement (20 mm vertical spacing).

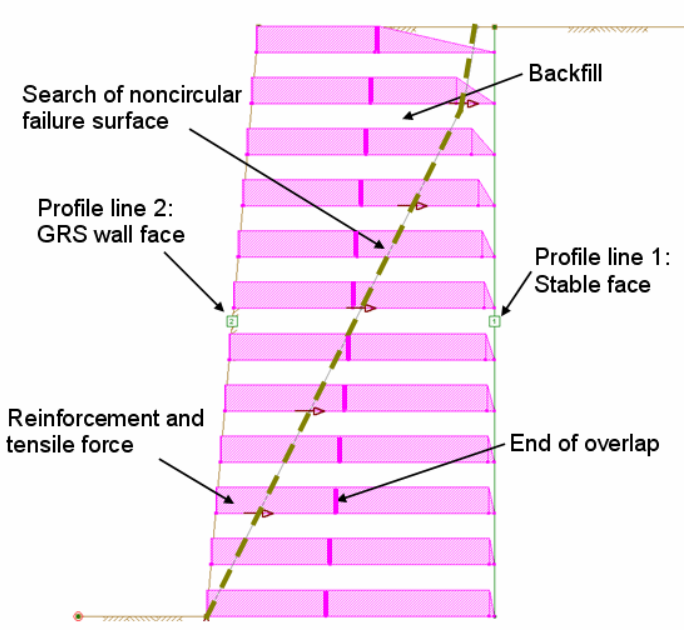

Figure 3. Limit equilibrium model of wall Test 2b

The stable wall face was assigned material properties such that it had theoretically infinite strength (very strong material). Because the existing wall is assumed "stable", the infinite strength of stabilized wall precludes failure surfaces passing through the stable face and constrained the search of the critical failure surface only within the GRS wall. Material model of the backfill in GRS wall was selected following a conventional Mohr-Coulomb model. Monterey No. 30 sand with relative density of 70 was characterized by unit weight of 16.05 kN/m^3, plane strain friction angle of 42.2° and zero cohesion. The centrifugal force was simulated by increasing the unit weight of backfill by N times corresponding to the target g-level.; for example, the unit weight for the modeling of centrifugal force at 41g was computed as 658.05 kN/m^3 (=16.05*41).

3.2 Modeling of Reinforcement

The forces in the reinforcement are limited by its ability to resist failure by rupture and by pullout as shown in Fig. 4. The way of modeling rupture and pullout resistance of the reinforcement is discussed below.

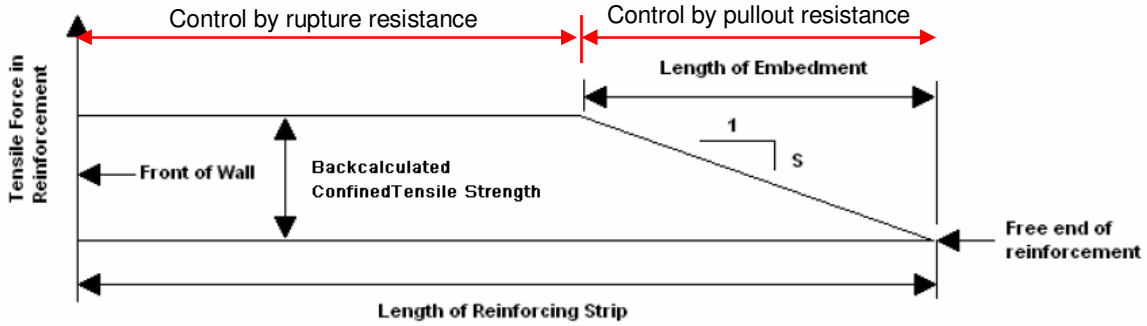

Figure 4. Schematic of assumed distribution of tensile stresses in the reinforcement

3.2.1 Tensile Forces

For the limit equilibrium analyses, the resistance of the reinforcement against failure by rupture was assumed to be the same for all layers of reinforcement as similar reinforcing material was used in each layer. Wide width strip tensile tests (ASTM D4595) showed the unconfined tensile strength of reinforcements used in Test2b was 0.09 kN/m. The reinforcement tensile strength under confinement was back-calculated based on the confined tensile strength for each centrifuge tests by force equilibrium analysis. The average confined tensile strength reported based on this analysis was 2.5 times larger than the unconfined tensile strength of reinforcements. Consequently, a confined tensile force 0.225 kN/m (=0.09*2.5) was used as the tensile strength in each layer of reinforcements.

3.2.2 Pullout Resistance

The pullout resistance of the reinforcement was assumed to increase linearly from zero at the free end of the reinforcement to a value equal to the tensile strength of the reinforcement. Figure 4 illustrates the variation of the longitudinal force in the reinforcement. The rate of change in force with horizontal distance, shown as *S* in Fig. 4 can be evaluated by Eq.[1], which was derived based on FHWA design guidelines (Elias *et al*, 2001).

$$S = F^* C R_c \alpha_v \sigma_{ov} \qquad [1]$$

where: F^* is the pullout resistance factor; C is the reinforcement effective unit perimeter; R_c is the coverage ratio; α_v is a scale correction factor which accounts for nonlinear stress reduction; σ_{ov} is the vertical overburden stress acting on the reinforcement. The recommended equation for the pullout resistance factor F^* for geosynthetic reinforcement is defined in the current FHWA design guidelines for MSE walls as 2/3*tan(ϕ), where ϕ is the backfill friction angle. Based on this recommendation and a friction angle of 42.2° used in Woodruff's centrifuge test, the value of F^* was adopted as 0.60. The effective unit perimeter of the reinforcement, C, was assigned a value of 2 to account for the top and bottom face of the reinforcements. The coverage ratio, R_c, for geosynthetic reinforcement is 1 because the reinforcement is a uniform sheet of material. The correction factor α_v depends primarily upon the strain softening of the compacted granular backfill material, the extensibility and the length of the reinforcement; it can be substantially smaller than 1 for extensible reinforcements. FHWA design guidelines recommends α_v of 0.6 for geotextiles. σ_{ov} is the vertical overburden stress acting on the reinforcement. When the aspect ratio is low, several studies (Frydman and Keissar, 1987; Take and Valsangkar, 2001; Leshchinsky and Hu, 2003; Lawson and Yee, 2005; Kniss *et al.*, 2007; Yang and Liu,2007) have

showed arching effect will reduce the vertical and horizontal earth pressures. This arching effect was included in σ_{ov} as follows:

$$\sigma_{ov} = \gamma z \beta_v \quad [2]$$

where: γ is the unit weight of the reinforced backfill; z is the depth of the layer of reinforcement below the top of the backfill; β_v is the vertical stress influence factor. Kniss *et al.*, 2007 conducted a series of finite element simulations to study the effect of arching effect on the vertical and horizontal stresses. The values of vertical stress influence factors β_v varying with wall aspect ratios are shown in Fig 5. For the case of wall aspect ratio 0.4 in Test 2b, a value of 0.65 was selected based on Fig. 5 to represent the average value of vertical stress influence factor between top and bottom layers. The final distribution of tensile forces of the reinforcements is shown in Fig. 3.

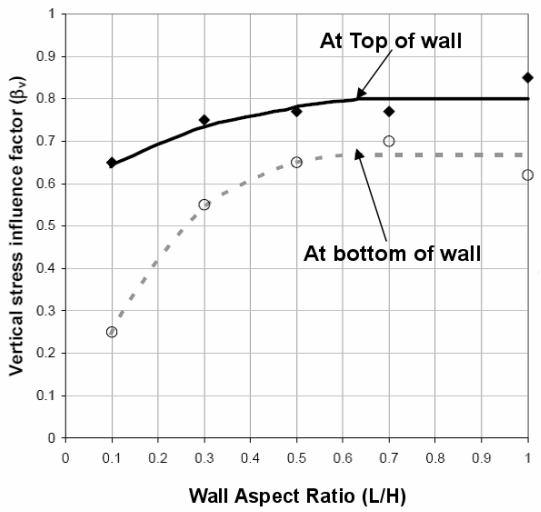

Figure 5. Vertical stress influence factors at the top and bottom of the wall (Kniss *et a*l., 2007)

3.2.3 Overlap Layer of Reinforcement

The reinforcements were wrapped around the wall face. The experimental results showed that this wrap-around (or overlapping) configuration increased the stability of the system. Consequently, the contribution of the geotextile overlap layers to the stability of the models was incorporated in the limit equilibrium models. The tensile force in the overlap layer was modeled using confined tensile force constantly through the entire overlap layer. The length of reinforcement was inputted as 50 mm, which corresponds to the length of the overlap layers in the centrifuge test.

3.2.4 Orientation of Reinforcement Tension

The resistance provided by the reinforcement is characterized in terms of longitudinal and transverse forces at selected points along each layer of reinforcement. The longitudinal force represents the resistance in the reinforcement parallel to the length of the reinforcement and the transverse force represents the resistance in the reinforcement perpendicular to the length of the reinforcement. However, it was assumed that the reinforcement only provides resistance in the longitudinal direction and the resistance in the transverse direction was assumed to be zero.

3.3 Search for Noncircular Failure Surface

Limit equilibrium calculations were performed using Spencer's method (Spencer 1967). This method satisfies all equilibrium conditions, *i.e.*, vertical force, horizontal force and moment equilibrium. The interslice forces were assumed to be parallel to each other. This assumption is required to balance the number of unknown parameters and the number of equilibrium equations. The vertical stress reduction due to arching effect is neglected for calculating the stress on the base of each hypothetical slice in Spencer's method. It is because the arching effect is most influential along the interface between stable face and narrow wall where the soil-structure interaction is most significant. The arching effect becomes less influential toward center line of narrow wall. In addition, it is also to avoid double taking account of the arching effect for both soil and reinforcement.

Limit equilibrium analyses in this study were performed using a search for a noncircular failure surfaces. Kniss *et. Al.* (2007) concluded that the noncircular failure surfaces are more critical than circular failure surfaces. In addition,

Woodruff (2003) also observed that the critical failure surface of a narrow wall showed a bilinear rather than circular shape. The searches for the noncircular failure surfaces were initiated by specifying the initial location of selected points along the failure surface. Kniss *et. al*, (2007) performed a parametric study to find the adequate number of points to define the initial failure surface. The study showed that an initial failure surface defined by from five to nine points is adequate. The seven points, evenly distributed through the height of the wall, were selected to define the initial failure surface. In all analyses, the first point on the initial failure surface was fixed at the toe of the wall. The last point was placed at the crest of the GRS wall. Fixing the first point at toe forced the failure surface to pass through this point, but other points on the initial failure surface were only allowed to move horizontally.

4. RESULTS

The results obtained based on the analyses conducted on the three centrifuge tests are presented in this section. The factor of safety at failure and the location of failure surface are the two most important results obtained from limit equilibrium analysis. In addition, these results are compared to the experimental results from centrifuge testing.

4.1 Factor of Safety versus G-Level

Figure 6 shows the calculated factor of safety as a function of the g-level for Test 2b (L/H =0.4) as obtained using limit equilibrium. The factor of safety decreases with increasing g-level. Figure 6 also shows that the wall is predicted to fail (FS=1) around 41.5g. Centrifuge testing indicated the wall failed at approximately 41g. Consequently, the g-levels at failure from centrifuge testing and limit equilibrium simulation are in a good agreement. Limit equilibrium simulation of Tests 2a (L/H=0.6) and 3a (L/H=0.7) exhibit similar trends. Wall is predicted to fail at 40g for both tests. Centrifuge testing indicated the wall failed at 39g for Test 2a and at 38g for Test3a. Both simulations show a close agreement with the g-levels at failure from centrifuge testing.

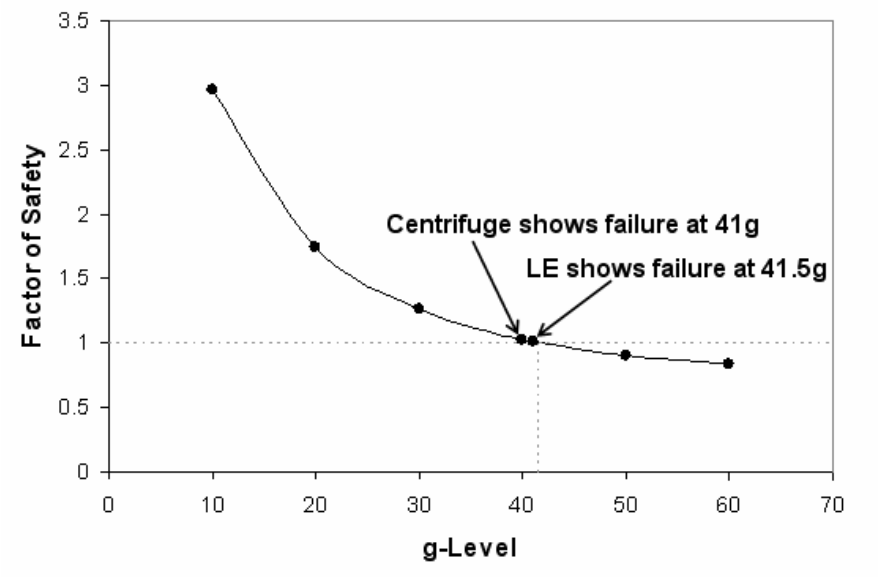

Figure 6. Factor of safety versus g-level for Test 2b

4.2 Location of the Failure Surface

In reinforced soil structures, the portion of the reinforcement that extends beyond the failure surface provides resistance against pullout. Therefore, location of failure surface is important to determine the pullout resistance of the reinforcement and eventually for the design of these structures. Figure 7a shows a comparison between the location of the failure surface obtained experimentally from Test 2b, and the one obtained using limit equilibrium analysis. Both the experimental and predicted results show the failure surface goes partially through the reinforced soil and partially along the interface between the reinforced soil and stable face. Finally, the inclination angle of the failure surface is less than the theoretical value defined by the Rankine failure surface criterion. Figures 7b and 7c show the comparison for Test 2a and Test 3a. Good agreements are also observed. Only a little discrepancy happens at the top of the failure surface in Fig. 7b; the predicted failure surface did not go along the interface near the top of the wall as shown by the experimental results.

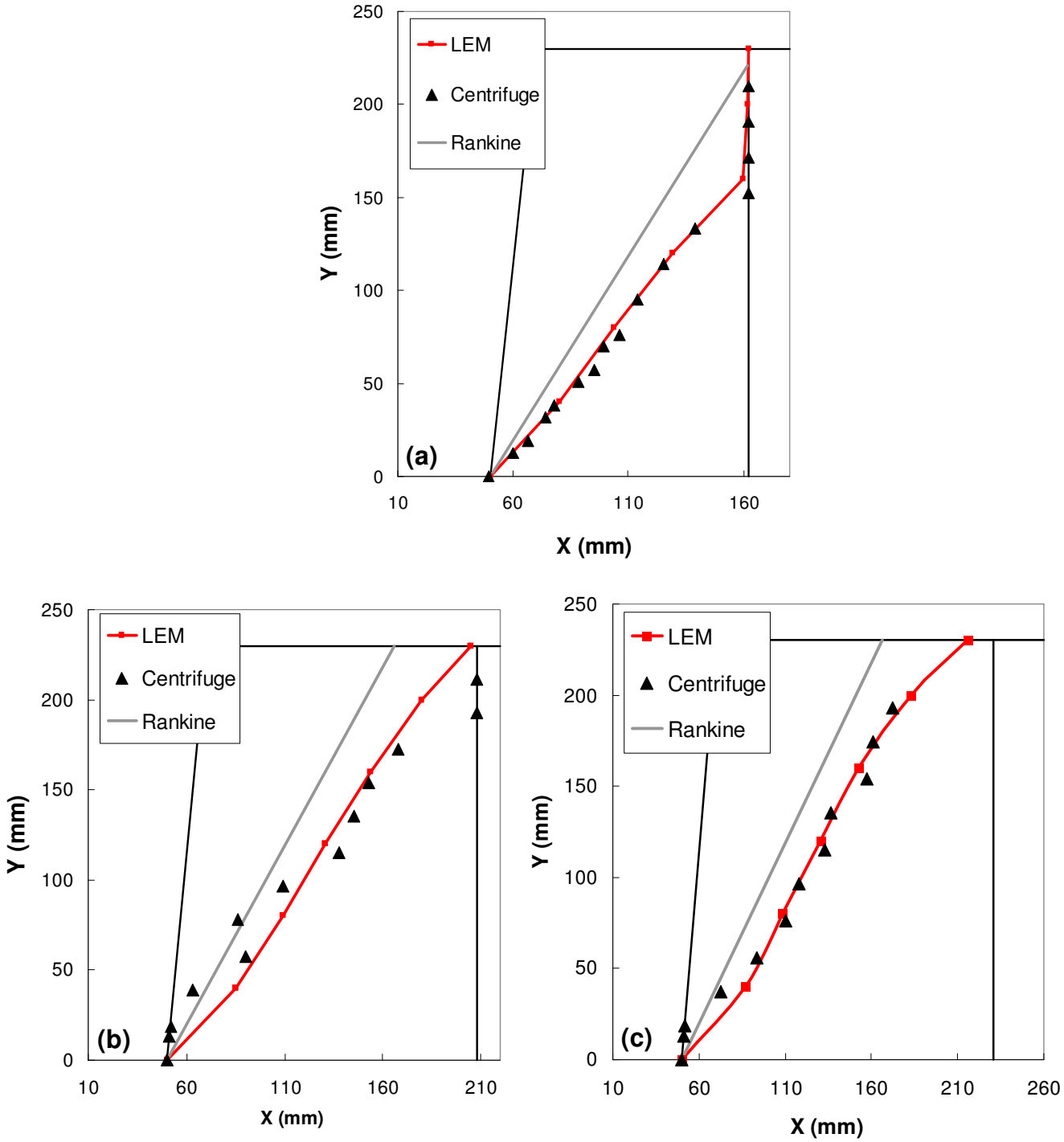

Figure 7. Location of failure surface for (a)Test 2b (*L/H*=0.4); (b) Test 2a (*L/H*=0.6); (c) Test 3a (*L/H*=0.7)

5. Effect of wall aspect ratio on failure plane

5.1 Design Chart: Inclination Angle of Failure Plane versus Wall Aspect Ratio

The inclination angle of the failure plane is an important parameter for calculating the *FS* against pullout. For the case of narrow GRS walls, the inclination angle is denoted as θ_f and illustrated in Fig. 8.

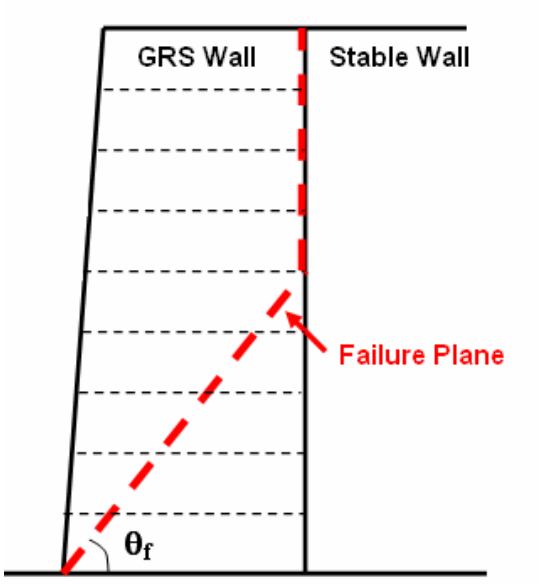

Figure 8. Define inclination angle of failure plane

The inclination angles of failure surfaces from Tests 2a, 2b, and 3b were measured based on the approach described above. Both of the results from centrifuge test and limit equilibrium analysis are shown in Fig. 9. The obtained inclination angles were normalized by the inclination angle of theoretical Rankine failure plane, $45+\phi/2$. A parametric study of the inclination angle of failure surface at L/H=0.3 was conducted. Figure 9 also includes an extra data point of centrifuge test reported by FHWA design guidelines for shored mechanically stabilized earth (SMSE) wall systems (Morrison *et al.*, 2006). This data point seems to follow the trend predicted by Woodruff (2003) centrifuge tests and limit equilibrium analyses. In addition, although Woodruff (2003) observed that when the wall aspect ratio decreased below 0.25, the failure mode changed from compound failure to external failure; in some cases, even though wall aspect ratio below 0.25 but the external failure is not going to happen. This may be because the external failure can be prevented by mechanically or frictionally connecting reinforcements to the shored wall. Therefore, the wall aspect ratio (x-axis in Fig. 9) is extended to a value of 0.2. The intension is to include the failure surface of wall aspect ratio from 0.2 to 0.3 for the cases discussed above.

Figure 9 shows a trend of inclination angles decreasing with the decrease of aspect ratios. This trend is characterized by a best-fit regression line using data from limit equilibrium analyses. The dashed horizontal line represents the inclination angle of Rankine failure plane suggested by FHWA SMSE wall design guidelines. The inclination angle suggested by FHWA SMSE wall design guidelines based on Rankine failure plane appears to overestimate the inclination angle of failure surface observed from centrifuge tests and limit equilibrium analyses. This would lead the estimating embedment length of reinforcement and the calculated factor of safety against pullout on unconservative side.

5.2 Possible Factors Affect Inclination Angle of Failure Surface

The reason for the difference in the failure surface from theoretical Rankine failure plane can be attributed to the following three factors:

1. Arching Effect (Interaction with Stable Face)
2. Boundary Constraint (Reduced Aspect Ratio)
3. Presence of Reinforcement

These factors not only constraint the degree of freedom of the soil mass but also interact with soil failure wedge by applying an extra vertical shear force on it (Filz and Duncan, 1997a and 1997b); thereby, the internal failure mechanism of GRS wall can not be easily predicted by Rankine theory (simply based on the Mohr-Column circle with vertical and horizontal principal stresses). For example, as shown in Fig. 9, because of the presence of stable face in narrow GRS wall systems, the normalized inclination angle is less than 1.0 even at L/H=0.7, which has enough space for failure plane to fully develop as Rankine linear failure plane. Moreover, the effect of aforementioned three factors will become amplified as the decrease of aspect ratio; this amplification reflects the decrease of normalized inclination angle as the decrease of aspect ratio shown in Fig. 9.

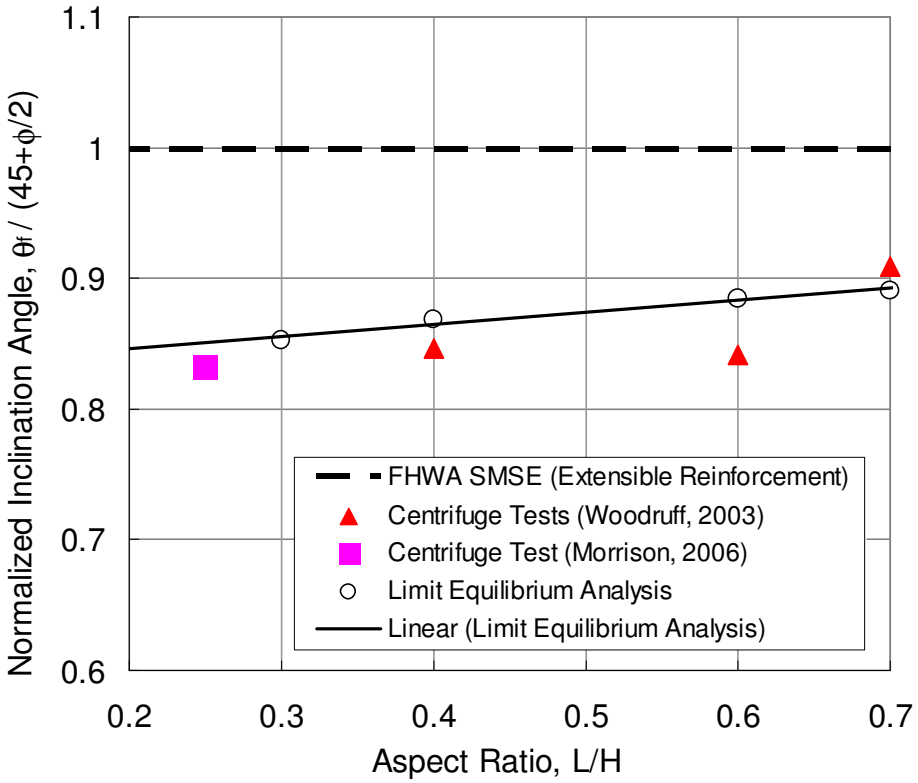

Figure 9. Normalized inclination angles

6. DESIGN IMPLICATION

The wall failure mode is a compound failure for a narrow wall with aspect ratio from 0.6 to 0.3. Due to the nature of compound failure mode (illustrated in Fig. 10a), the failure surface (pink line) will not intersect with upper layer reinforcements (blue dashed lines from reinforcement layer number 7 to 10). The effect of reinforcing backfill through developed tensile force should not be counted for those layers of reinforcements without the intersection with failure surface. One can envision the narrow wall system in Fig. 10a as identically to that in Fig 10b. Only the lower reinforcement layers (*i.e.*, those that extend into the resistant zone) are designed to resist breakage and pullout for the entire "active" MSE mass.

For the situation addressed above, FHWA SMSE wall design guidelines (Morrison *et al.*, 2006) recommends to check a overall pullout stability ($FS_{p,,overall}$) in addition to conventional internal stability evaluations (*i.e.* breakage and pullout stability for each individual layer of reinforcement). For the same reason, this study suggests to include a overall breakage stability ($FS_{b,overall}$) into the internal stability evaluations as well . Eq. [3] and Eq. [4] are the formulas used to evaluate the overall stabilities against breakage and pullout, respectively. The idea is to divide the summation of all resistant force by the summation of all driving force.

$$FS_{b,overall} = \frac{\Sigma_{i=1}^{i=j} T_{al,,i}}{\Sigma_{i=1}^{i=j} T_{\max,,i}} \quad [3]$$

$$FS_{p,overall} = \frac{\Sigma_{i=1}^{i=j} Pr_i}{\Sigma_{i=1}^{i=j} T_{max,i}} \quad [4]$$

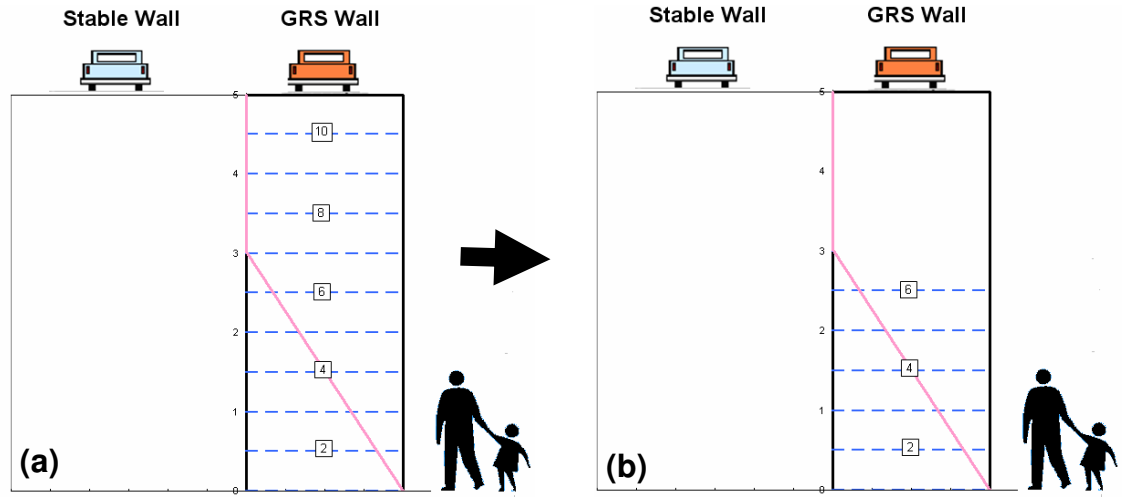

Figure 10. Illustration of two conceptually identical systems:
(a) with upper layer reinforcements; (b) without upper layer reinforcements

where; T_{al} is the allowable reinforcement tensile strength; T_{max} is the maximum tension developed in reinforcement; P_r is the pullout capacity; i is i^{th} layer of reinforcement, i∈ [1,2,3,…j]; j is the number of reinforcement layer that satisfies pullout criteria ($FS_{p,i}$>1.5) at each reinforcement layer. T_{max} can be calculated as earth pressure times vertical spacing of reinforcements in conventional walls. As for T_{max} in narrow walls, the earth pressure will be reduced due to arching effect and boundary constraint. T_{max} can be estimated as Eq. [5]

$$T_{max} = \gamma z K_a R_d \cdot S_v \quad [5]$$

where: γ is the unit weight of the reinforced backfill; z is the depth of the layer of reinforcement below the top of the backfill; K_a is the active earth pressure coefficient; S_v is vertical spacing of reinforcements; R_d is the reduction factor to account for arching effect and boundary constraint. Readers are referred to Kniss et. al. (2007) and Yang and Liu (2007) for more detail. P_r can be estimated by multiplying S (in Eq. [1]) and reinforcement embedment length L_e together. Note P_r should be less than T_{al}. Reinforcement embedment length L_e can be evaluated as Eq. [6].

$$L_e = L - \frac{h}{tan\,\theta_f} \quad [6]$$

where; L is wall width; h is reinforcement elevation, θ_f is the inclination angle of failure surface. θ_f is depended on wall aspect ratio and can be evaluated using Fig. 9.

SUMMARY

This paper presented a limit equilibrium study to locate failure planes within narrow GRS walls. Limit equilibrium analyses were used to model the centrifuge test of narrow GRS walls. The forces in geosynthetic reinforcement for narrow MSE walls were discussed. The predicted results were in agreement with the centrifuge experimental results. The results indicated that critical failure plane was bilinear. The failure surface formed partially through the reinforced soil and partially along the interface between the GRS and stable wall faces. In addition, the inclination angle of the critical failure plane decreased with the decrease in wall aspect ratio. The calibrated limit equilibrium model was then used as the basis for the design of other narrow GRS walls. This study concluded that using the inclination angle as obtained using Rankine failure plane for narrow wall systems results in an overestimation of the actual inclination angle. Thus a new design chart for inclination angle of failure surface versus various wall aspect ratios was proposed. This design chart provided the information on the location of the failure surface and the embedment length of reinforcement needed to calculate the factor of safety against pullout. Finally the design implications related to overall internal stability based on the revised analysis were discussed.

ACKNOWLEDGEMENTS

The work of limit equilibrium analysis was greatly consulted and helped by Dr. Stephen Wright, the author of UTEXAS4 program. The First author is indebted to his Colleague, Ken Kniss, for his preliminary simulations. Comments from reviewers and editors to improve the clarity and quality of paper are appreciated.

REFERENCES

Elias, V., Christopher, B.R., and Berg, R.R., (2001), "Mechanically Stabilized Earth Walls and Reinforced Soil Slopes Design and Construction Guidelines," *Report No. FHWA-NHI-00-043*, Federal Highway Administration.

Filz, G.M., and Duncan, J. M. (1997a). "Vertical Shear Loads on Nonmoving Walls. I: Theory," *Journal of Geotechnical and Geoenvironmental Engineering,* ASCE*,* Vol. 123, No. 9, pp.856-862.

Filz, G.M., and Duncan, J. M. (1997b). "Vertical Shear Loads on Nonmoving Walls. II: Application," *Journal of Geotechnical and Geoenvironmental Engineering,* ASCE*,* Vol. 123, No. 9, pp.863-873.

Frydman, S. and Keissar, I., (1987) "Earth Pressure on Retaining Walls near Rock Faces," *Journal of Geotechnical Engineering,* ASCE*,* Vol. 113, No. 6, June, pp. 586-599

Kniss, K., Wright, S., Zornberg, J.G., and Yang, K.-H., "Design Considerations for MSE Retaining Walls Constructed in Confined Spaces" *Center for Transportation Research (CTR), Report no. 0-5506-1,* Austin, Texas, October 2007.

Lawson, C.R., and Yee, T.W., (2005), "Reinforced Soil Retaining Walls with Constrained Reinforced Fill Zones" *Proceedings*, *GeoFrontiers 2005*, ASCE Geo-Institute Conference, pp. 2721-2734.

Leshchinsky, D., Hu, Y. and Han, J., (2004) "Limited Reinforced Space in Segmental Retaining Wall," *Geotextiles and Geomembranes*, Vol. 22, No. 6, pp. 543-553.

Morrison, K.F., Harrison, F.E., Collin, J.G., Dodds, A., Arndt, B. (2006), "Shored Mechanically Stabilized Earth (SMSE) Wall Systems Design Guidelines," *Report No.FHWA-CFL/TD-06-001,* Federal Highway Administration.

Spencer, E (1967). "A Method of Analysis of the Stability of Embankments Assuming Parallel Inter-Slice Forces". *Geotechnique*, 24(4), p. 661-665.

Take, W.A. and Valsangkar (2001), "Earth Pressures on Unyielding Retaining Walls of Narrow Backfill Width," *Can. Geotech. Journal,* Vol.38, pp.1220-1230.

Woodruff, R. (2003), "Centrifuge Modeling of MSE-Shoring Composite Walls," *Thesis*, the Univ. of Colorado, Boulder.

Wright, S.G. (1999), "UTEXAS4 A Computer Program for Slope Stability Calculations." Shinoak Software, 221p.

Yang, K-H and Liu, C-N (2007), "Finite Element Analysis of Earth Pressures for Narrow Retaining Wall", *Journal of GeoEngineering.*, Taiwan Geotechnical Society, 2(2): 43-52.

Zornberg, J.G., Sitar, N., Mitchell, J.K. (1998). "Limit Equilibrium as Basis for Design of Geosynthetic-Reinforced Slopes." *Journal of Geotechnical Engineering*, 124 (8), p.684-698.

Zornberg, J.G. (2002). "Peak versus Residual Shear Strength in Geosynthetic-Reinforced Soil Design", *Geosynthetic International*, Vol. 9, No. 4, pp 387-389.